

Viscoelasticity of Dynamically Self-Assembled Paramagnetic Colloidal Clusters

Pietro Tierno, Ramanathan Muruganathan, and Thomas M. Fischer*

Department of Chemistry and Biochemistry, Florida State University, Tallahassee, Florida 32306, USA
(Received 1 June 2006; published 9 January 2007)

Paramagnetic particles in a liquid above a solid dynamically self-assemble into two-dimensional (2D) viscoelastic clusters in a precessing magnetic field if the precession angle exceeds the magic angle. Hexagonal clusters rotate with a frequency proportional to the precession frequency of the magnetic field. The rotation is explained by viscoelastic shear waves excited in the clusters that can be visualized slightly above the magic angle. The cluster rotation and the visualization of viscoelastic modes are independent techniques to probe the rheological properties of the cluster. We find agreement between both techniques when determining the 2D cluster viscosity $\eta_c \approx 10^{-11}$ N s/m.

DOI: 10.1103/PhysRevLett.98.028301

PACS numbers: 83.80.Hj

Many important natural systems, from humans to bacterial colonies to weather patterns, require a continuous dissipation of energy to be dynamically sustained in their actual complex structure [1]. Ensembles of small polarizable objects under dynamic external fields provide one simplified laboratory scale model system for dynamic self-assembly [2–9]. Even simple systems like two paramagnetic particles [4], or two magnetic holes [5,6] in a rotating magnetic field dynamically self-assemble into doublets. The doublets rotate in the surrounding liquid with a frequency below the frequency of the rotating magnetic field. The instantaneously induced dipolar forces favor an assembly of paramagnetic particles into pearl chains [7]. For sufficiently low frequencies the hydrodynamic friction cannot prevent the chains, doublets or asymmetric clusters from permanently aligning and rotating with the rotating magnetic field. However symmetric assemblies, such as ferrofluid drops [8,9], also rotate in a precessing field. Thus a different mechanism should be responsible for the rotation of symmetric clusters.

Here we focus on the dynamic self-assembly of symmetric 2D colloidal clusters. First we show that few paramagnetic particles, initially arranged in a colloidal liquid, can dynamically self-assemble into a viscoelastic solid cluster. Then we show that viscoelastic shear waves excited in the clusters are the base mechanism for the cluster rotation. This provides understanding of dynamic self-assembly of paramagnetic particles into symmetric clusters and also enables probing the cluster's rheological properties.

We used polystyrene paramagnetic particles with a radius $a = 1.4 \mu\text{m}$ and an effective magnetic susceptibility $\chi_{\text{bead}} = 0.17$ (Dynabeads M-270). A water drop containing $\sim 7 \times 10^6$ beads/ml was placed on a glass plate. The particles sediment above the glass-water interface, then float a few nanometers above the surface because of the electrostatic repulsion between the negatively charged particles (COO^- group) and the negative glass surface caused by dissociation of the silanol groups [10].

By tracking an individual colloidal particle we determined the particle diffusion coefficient as $D = 0.14 \pm 0.05 \mu\text{m}^2/\text{s}$, from this we estimated the hydrodynamic drag coefficient as $f_{\text{bead}} = k_B T / \eta_w a D \approx 27.7$ where k_B is Boltzmann's constant, T the temperature, and η_w is the viscosity of the water [11]. Three coils with the main axes along the x , y , and z directions were used to produce a magnetic field up to $H \sim 0.5 \times 10^5$ A/m in each direction and precessing with an angular frequency Ω at an angle ϑ with respect to the axis normal to the glass plate (see Fig. 1). The particles were observed by using an optical

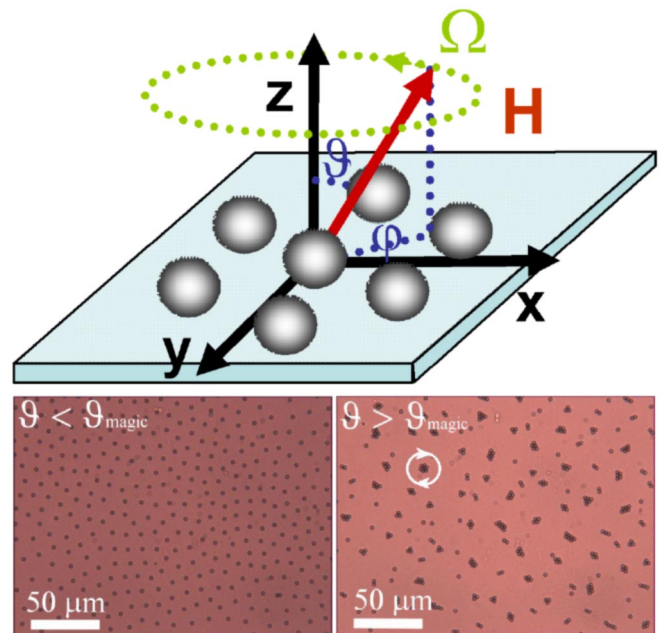


FIG. 1 (color online). Schematic showing a hexagonal cluster in a precessing field \mathbf{H} of angular frequency Ω . In the bottom line are 2 microscope images of a liquid colloidal assembly with $\vartheta < \vartheta_{\text{magic}}$ ($\vartheta = 52.9^\circ$, $H = 2693$ A/m) and an assembly of nucleated colloidal clusters with $\vartheta > \vartheta_{\text{magic}}$ ($\vartheta = 90.0^\circ$, $H = 2148$ A/m) that rotate in the precessing field. Here $\vartheta_{\text{magic}} = 54.7^\circ$ and $\Omega = 352 \text{ s}^{-1}$.

microscope (Leica, DMLP), and videos for image analysis were taken either at 250 fps (Fastcam Super 10 K Photron), or at 30 fps (Basler A311F, color camera).

In the absence of a magnetic field, or in a field precessing with an angle $\vartheta \leq \vartheta_{\text{magic}}$ ($\vartheta_{\text{magic}} = 54.7^\circ$ is the zero of the second Legendre polynomial $P_2(\cos\vartheta_{\text{magic}}) = 0$), the floating particle formed a 2D liquid (number density $n_s \sim 10^{10} \text{ m}^{-2}$) in the xy plane. Application of a precessing magnetic field ($\Omega \gg 10 \text{ s}^{-1}$, $\vartheta > \vartheta_{\text{magic}}$) leads to the formation of small rotating 2D solid clusters, like doublets, triangles, squares, or hexagons, separated from each other by a phase depleted of colloidal particles (Fig. 1 bottom right).

The dynamic cluster assembly can be explained in terms of the time-averaged dipolar interactions between the individual induced magnetic dipoles and the repulsive stabilizing (electrostatic or steric) interaction between the particles of the cluster. In the cluster interior, the dipolar interaction arising from opposite neighboring particles cancel each other. The only particles feeling a significant dipolar force are those located at the border of the cluster. In published work on the effect of dipolar interactions on patterns in 2D monolayers, or ferrofluid films, the interactions vanish in the bulk and their effect can be expressed with a continuum description in terms of a dipolar line tension λ [12,13], that is a 2D analog of the surface tension in 3D systems. Since the induced magnetic moments of the particles are tilted with respect to the normal to the glass surface, the dipolar line tension of our cluster consists of an isotropic part and an anisotropic part:

$$\lambda_{\text{dip}} = \lambda_{\text{is}} + \lambda_{\text{anis}} \cos 2\phi, \quad (1)$$

where ϕ is the angle between the in-plane magnetic field and the in-plane vector \mathbf{n} , normal to the 2D cluster boundary. At high frequencies of the precessing magnetic field the angle ϕ rotates with the frequency of the field and the cluster cannot follow this fast rotation. The isotropic line tension is the only contribution that remains after time averaging. Magic angle spinning nuclear magnetic resonance (MAS-NMR) is a well-known technique for time averaging the nuclear dipole interactions to zero, and to narrow NMR peaks by spinning the sample at the magic angle around the magnetic field. Here we spin the *magnetic field* around the sample. Similar effects to those in MAS-NMR make λ_{is} of our colloidal clusters vanish at ϑ_{magic} . We find that $\lambda_{\text{is}} \propto -H^2 P_2(\cos\vartheta)$, such that $\lambda_{\text{is}} < 0$ for $\vartheta < \vartheta_{\text{magic}}$ and $\lambda_{\text{is}} > 0$ for $\vartheta > \vartheta_{\text{magic}}$. The effect of the time-averaged dipolar interactions is a negative line tension which destabilizes the cluster for $\vartheta < \vartheta_{\text{magic}}$. Consequently, we observe a homogeneous distribution of particles for $\vartheta < \vartheta_{\text{magic}}$ (Fig. 1, bottom left). For angles exceeding the magic angle a positive tension compresses the colloidal particles to form closed packed solid clusters (Fig. 1, bottom right). The tension pulls the particles together until repulsive electrostatic or steric interactions balance the compressive effect. The particles dynamically

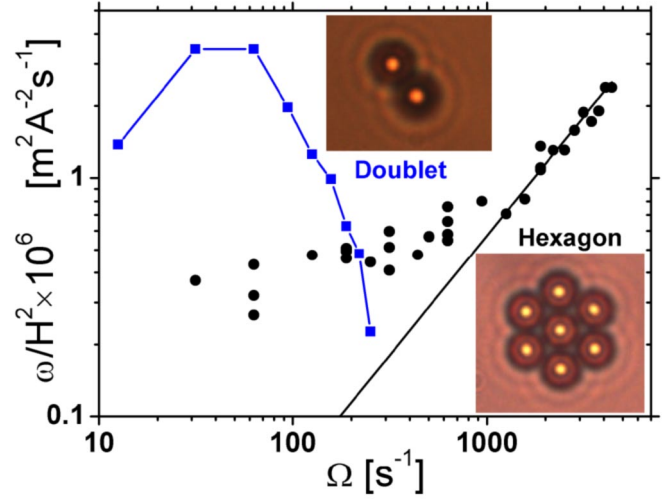


FIG. 2 (color online). Normalized cluster rotation frequency as a function of the angular frequency of the external field for $\vartheta = 90.0^\circ$. The blue (or gray) squares refer to a doublet of paramagnetic particles and the black circles to the hexagon. The continuous black line is a fit using Eq. (5). A video of a rotating hexagon and a nonrotating doublet can be viewed in [13].

self-assemble into a solid cluster of radius R_c and we expect the cluster to acquire a shear modulus $G'_c \approx \lambda_{\text{is}}/R_c$ that is of the order of the pressure compressing the cluster.

In Fig. 2 we show the normalized cluster rotation frequency ω/H^2 as a function of the angular frequency of the magnetic field Ω for a doublet (squares) and for a hexagonal cluster (circles) for precession in-plane ($\vartheta = 90^\circ$). At low frequency, doublets rotate faster than hexagons and synchronously with the precessing field. For increasing frequencies, higher than $\sim 100 \text{ s}^{-1}$, the doublets are not able to follow the field dynamics and asynchronously rotate with lower and lower rotation frequency until they stop rotating at rates higher than $\sim 250 \text{ s}^{-1}$. Conversely, hexagons rotate with a frequency proportional to the square of the external field, itself increasing with the precession frequency. A movie of the motion can be viewed in [13]. The rotation of doublets and longer chains has been shown to be due to the anisotropy of the magnetic susceptibility tensor [4–7]. For symmetry reasons the magnetic susceptibility tensor of hexagonal clusters is isotropic. Our experiments therefore suggest, that the cluster rotation of the hexagon at high frequencies originates from a mechanism which is absent in the doublets and longer particle chains. Doublets and chains, in contrast to larger clusters, are 1D assemblies that cannot be shear deformed. We will show that dissipative shear deformations, traveling around the cluster with the frequency of the precessing magnetic field, cause the cluster rotation observed at high precession frequencies.

For the cluster of volume V_c to rotate, a finite magnetic torque $\tau_{\text{magn}} = \mu_0 V_c \mathbf{M} \times \mathbf{H}$, is required to counteract the viscous torque $\tau_{\text{visc}} = f \eta_w R_c^3 \omega$ arising from the rotation

of the cluster inside the viscous liquid (of viscosity η_w). Here μ_0 is the permeability of vacuum, f the dimensionless drag coefficient of the cluster [14], $\mathbf{M}(t) = \int_{-\infty}^t dt' \chi_{\text{eff}}(t-t') \mathbf{H}(t')$ is the cluster magnetization and χ_{eff} is the effective dynamic magnetic susceptibility tensor. A finite torque only arises when the magnetization \mathbf{M} and magnetic field \mathbf{H} are linearly independent vectors. In a rotating magnetic field, doublets and longer chains of paramagnetic particles rotate because the major axes of their anisotropic susceptibility tensors lag behind the magnetic field [7,9] and cause \mathbf{M} and \mathbf{H} to point in different directions. However, in a dynamic magnetic field the magnetization \mathbf{M} of the object can be linearly independent of the magnetic field, even if the susceptibility is isotropic, because the magnetization is collinear to the magnetic field from a preceding time. For an hexagonal cluster having an isotropic susceptibility tensor, only the memory effect of the susceptibility can cause a rotation. We find a magnetic torque $\tau_{\text{magn}} = \mu_0 V_c H^2 \sin^2 \vartheta \chi_{\text{eff}}'' \mathbf{e}_z$ that is proportional to the imaginary part of the isotropic dynamic magnetic susceptibility $\chi_{\text{eff}}''(\Omega - \omega)$, with the frequency of rotation $\Omega - \omega$ of the field in the reference frame of the cluster. The cluster rotates due to internal relaxation processes that manifest themselves as peaks in $\omega \propto \chi_{\text{eff}}''(\Omega - \omega)$. The precession frequency causing a peak in χ_{eff}'' and hence in ω , should be comparable to the relaxation rate of the internal cluster relaxation process. In a single paramagnetic colloidal particle typical relaxation frequencies of, e.g., Néel relaxations, are in the order of GHz, which are too large to cause significant values of $\chi_{\text{eff}}''(\Omega - \omega)$ in the quasistatic regime $\Omega \approx 1\text{--}100 \text{ s}^{-1}$. In paramagnetic colloidal clusters, however, the viscoelastic cluster relaxation processes have relaxation rates of the order $\gamma_c \approx \mu_0 a_{\text{bead}}^2 \chi_{\text{bead}}^2 \hat{H}^2 / \eta_c R_c \approx 10 \text{ kHz}$, where η_c is the effective 2D viscosity of the cluster. The rotation frequency data of the hexagon in Fig. 2 is hence the low Ω wing of the viscoelastic relaxation peak. Non symmetric clusters, thicker than colloidal chains, rotate due to both shape anisotropy and viscoelastic relaxation. The former effect dominating at low, the latter at high frequencies.

To understand the rotation of the symmetric cluster we calculate the dynamic cluster deformation \mathbf{u} , caused by the dipolar interactions within the cluster. We consider the hexagonal cluster as a 2D incompressible viscoelastic continuum, satisfying the elasticity equation:

$$-\nabla p + G_c \Delta \mathbf{u} = 0 \quad (2)$$

where G_c is the shear modulus and $p > 0$ is the nonmagnetic (electrostatic or steric) pressure required to ensure the incompressibility of the cluster. Since the dipolar forces only act at the cluster boundary, they enter into (2) only via the boundary condition:

$$\frac{\partial(\lambda_{\text{dip}} \mathbf{t})}{\partial s} = \sigma \cdot \mathbf{n} \quad (3)$$

which states that the elastic stress normal to the boundary

is caused by the dipolar line tension gradient. In Eq. (3) \mathbf{t} , \mathbf{n} , and s denote the tangential vector, normal vector, and arclength to the cluster boundary, and $\sigma = -p\mathbf{1} + G_c(\nabla \mathbf{u} + (\nabla \mathbf{u})^\dagger)$ is the elastic stress tensor. Solving the Eq. (2), subject to the boundary condition (3) imposed by a precessing field, to first order in the deformation of the boundary, we predict a radial and azimuthal distortion of $u_r/R_c = -2\lambda_{\text{anis}} e^{-2i\phi} / 3(\lambda_{\text{is}} + G_c R_c)$, and $u_\phi/R_c = i\lambda_{\text{anis}} e^{-2i\phi} (3\lambda_{\text{is}} + 5G_c R_c) / 3G_c R_c (\lambda_{\text{is}} + G_c R_c)$ [13]. For a purely elastic solid, $G_c = G_c'$, this distortion is in phase with the magnetic field and hence cannot cause a rotation of the cluster. However, for a viscoelastic colloid, $G_c = G_c' - iG_c''$, where G_c'' is the loss modulus, the shear wave lags behind the magnetic field and can cause cluster rotation. The simplest model of a viscoelastic colloid is the Voigt-Kelvin model [15], with a frequency independent storage module and viscosity $G_c = \lambda_{\text{is}}/R_c - 2i(\Omega - \omega)\eta_c$. Using this model we predict a radial distortion

$$u_r/R_c = \frac{-\lambda_{\text{anis}}(\lambda_{\text{is}} + i(\Omega - \omega)\eta_c R_c)}{3(\lambda_{\text{is}}^2 + (\Omega - \omega)^2 \eta_c^2 R_c^2)} e^{-2i\phi}. \quad (4)$$

The distortion of the cluster creates a demagnetization anisotropy that lags behind the same amount the distortion lags behind. Hence we expect the loss part of the susceptibility to be proportional to the loss part of the shear modulus: $\chi_{\text{eff}}'' = 3\pi a u_r'' / 8R_c^2$. For small precession frequencies χ_{eff}'' increases linearly with the precession frequency. As a consequence, the rotation frequency of the hexagonal clusters increases linearly with the precession frequency:

$$\frac{\omega}{H^2} = \frac{27\pi\eta_c}{8\eta_w a H^2} \frac{(1 - P_2)^2}{9P_2^2} \frac{\ln(\frac{2^{5/2}R_c}{3^{1/4}e^{7/3}a})}{\ln^2(\frac{2^{5/2}R_c}{3^{1/4}ea})} \frac{\Omega}{f_{\text{bead}} \chi_{\text{bead}}^2}. \quad (5)$$

By fitting the normalized cluster rotation frequency of Fig. 2 with Eq. (5) we estimate the 2D viscosity as $\eta_c = 6.4 \times 10^{-12} \text{ N s m}^{-1}$. If we write the cluster viscosity as $\eta_c = d \cdot \eta_w$, where η_w is the water viscosity and d is a length, we obtain a value of $d \sim 6 \text{ nm}$ consistent with a minimum interparticle distance, as dictated by the electric double-layer interparticle repulsion. This *a posteriori* justifies the use of a continuum description even for an ensemble as small as seven particles. The major dissipation within the cluster occurs due to liquid shear fluxes in the region where the colloidal particles come close to each other. Equation (5) predicts that the cluster rotation frequency increases by decreasing the precession angle toward the magic angle. In Fig. 3, we test this prediction by plotting the normalized rotation frequency of the hexagonal cluster ω/H^2 as a function of $P_2(\cos\vartheta)$ for $\Omega = 63 \text{ s}^{-1}$ and find agreement with Eq. (5) when using the above cluster viscosity. Two movies in [13] show the slower and faster rotation of the hexagon at $\vartheta = 90^\circ$ and 58° .

Finally, we test our model by directly observing the shear deformation of the cluster. This is possible at an

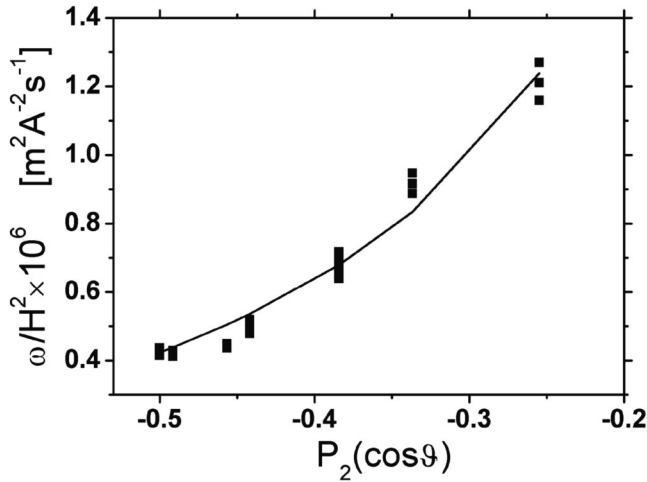


FIG. 3. Normalized cluster rotation frequency vs $P_2(\cos\vartheta)$ for $\Omega = 63 \text{ s}^{-1}$, where the continuous line is a fit to Eq. (5). Two movies showing the speeding up of the hexagon are in [13].

angle $\vartheta = 67^\circ$, slightly above the magic angle, since there the perturbation of the anisotropic time dependent line tension is large compared to the marginally stabilizing isotropic tension, resulting in large deformations. We recorded a high speed video (250 fps) of the cluster and took the Fourier transform of the elliptical mode as $u_r(\Omega') = \frac{1}{6} \sum_{j=1}^6 \frac{1}{T} \int_0^T e^{2i(\Omega't - \varphi_j)} r(\varphi_j, t) dt$, where $r(\varphi_j, t)$ are the separations of the six outer colloidal particles of the hexagon from the central one. In Fig. 4 we plot $u_r(\Omega')$ versus Ω' (inset) and in [13] we show a movie of a strongly deformed rotating hexagon. As expected, we observe a pronounced peak of the deformation at the frequency $\Omega' = 2(\Omega - \omega)$.

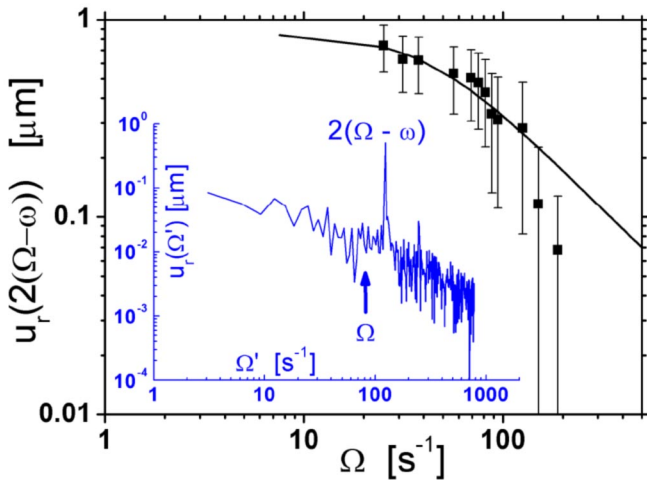


FIG. 4 (color online). Elliptic deformation u_r as a function of the frequency of the external magnetic field for $\vartheta = 67^\circ$. In the blue (or gray) inset on the left side we show the deformation in Fourier space for an angular frequency of 70 s^{-1} and $H = 2341 \text{ A/m}$. A movie of the elastic shear wave traveling around the rotating hexagon can be viewed in [13].

The strength of this peak is then plotted as a function of the precession frequency Ω (squares). A fit according to the absolute value of Eq. (4) (continuous line) yields a second independent way to determine the 2D cluster viscosity. In this case we find a higher 2D viscosity, $\eta_c = 8.6 \times 10^{-11} \text{ N s m}^{-1}$, since the separation $d \approx 100 \text{ nm}$ between the beads increases close to the magic angle. Since the value of d is determined by the range of the electric double-layer repulsion, adding salt should reduce the cluster viscosity by reducing the volume where the dissipation occurs. Indeed, performing the experiments in a 1 mM NaCl solution reduces the cluster rotation frequency by a factor of ~ 20 .

In summary, we have studied the dynamic self-assembly of small colloidal clusters in a precessing magnetic field. The assembly is driven by dipolar interactions that, on average, are attractive for precession angles above the magic angle. At the magic angle, the clusters undergo a liquid to solid transition, as determined from their elastic shear moduli. The rotation of symmetric hexagonal clusters is caused by dissipative elastic shear waves traveling around the cluster. Measurements of the clusters rotation frequencies give direct access to the viscoelastic properties of colloidal clusters.

We acknowledge discussions with Colin Byfleet.

*Electronic address: tfischer@chem.fsu.edu

- [1] G. M. Whitesides and B. Grzybowski, *Science* **295**, 2418 (2002).
- [2] M. Trau, D. A. Saville, and I. A. Aksay, *Science* **272**, 706 (1996).
- [3] B. A. Grzybowski, H. A. Stone, and G. M. Whitesides, *Nature (London)* **405**, 1033 (2000).
- [4] O. G. Calderón and S. Melle, *J. Phys. D* **35**, 2492 (2002).
- [5] A. T. Skjeltorp, *Phys. Rev. Lett.* **51**, 2306 (1983).
- [6] P. Pieranski, S. Clausen, G. Helgesen, and A. T. Skjeltorp, *Phys. Rev. Lett.* **77**, 1620 (1996).
- [7] S. L. Biswal and A. P. Gast, *Phys. Rev. E* **69**, 041406 (2004).
- [8] K. I. Morozov, A. Engel, and A. V. Lebedev, *Europhys. Lett.* **35**, 609 (1996).
- [9] J. C. Bacri, A. Cebers, and R. Perzynski, *Phys. Rev. Lett.* **72**, 2705 (1994).
- [10] S. H. Behrens and D. G. Grier, *J. Chem. Phys.* **115**, 6716 (2001).
- [11] L. E. Helseth, H. Z. Wen, T. M. Fischer, and T. H. Johansen, *Phys. Rev. E* **68**, 011402 (2003).
- [12] H. M. McConnell, *Annu. Rev. Phys. Chem.* **42**, 171 (1991).
- [13] See EPAPS Document No. E-PRLTAO-98-022703 for supplementary information and movies of hexagonal clusters. For more information on EPAPS, see <http://www.aip.org/pubservs/epaps.html>.
- [14] $f \approx 6f_{\text{bead}}a/R_c$ for a hexagon.
- [15] Sir. W. Thomson, *Proc. R. Soc. London* **14**, 289 (1865); W. Voigt, *Ann. Phys. (Leipzig)* **47**, 671 (1892).